

Cross Section Measurements of (n,x) Reactions at 17.9 and 18.9 MeV Using Highly Enriched Ge Isotopes

S. Chasapoglou^{1,*}, R. Vlastou¹, M. Kokkoris¹, M. Diakaki¹, V. Michalopoulou¹, G. Gkatis¹, A. Stamatopoulos¹, M. Axiotis², S. Harissopoulos², A. Lagoyannis², M.I. Savva³, I.E. Stamatelatos³, T. Vasilopoulou³, and C. Lederer-Woods⁴

¹ Department of Physics, National Technical University of Athens, 157 80 Athens, Greece

² Tandem Accelerator Laboratory, Institute of Nuclear and Particle Physics, NCSR Demokritos, 153 10 Aghia Paraskevi, Greece

³ Institute of Nuclear and Radiological Sciences, Energy, Technology & Safety, NCSR Demokritos

⁴ School of Physics and Astronomy, University of Edinburgh, United Kingdom

Abstract. Nine neutron induced reactions on Ge isotopes ($^{70}\text{Ge}(n,2n)^{69}\text{Ge}$, $^{76}\text{Ge}(n,2n)^{75}\text{Ge}$, $^{73}\text{Ge}(n,p)^{73}\text{Ga}$, $^{72}\text{Ge}(n,p)^{72}\text{Ga}$, $^{73}\text{Ge}(n,d/np)^{72}\text{Ga}$, $^{74}\text{Ge}(n,d/np)^{73}\text{Ga}$, $^{74}\text{Ge}(n,\alpha)^{71m}\text{Zn}$, $^{72}\text{Ge}(n,\alpha)^{69m}\text{Zn}$, $^{73}\text{Ge}(n,\alpha)^{69m}\text{Zn}$) have been measured in this work at energies 16.4-18.9 MeV. For these reactions, most of the experimental datasets in literature were obtained with a ^{nat}Ge target. However, the residual nucleus produced by some reaction channels can also be produced from neighboring isotopes, acting as a contamination for the measured reactions. This contribution must be subtracted, based on theoretical calculations, bearing their own uncertainties. The use of enriched targets however, does not suffer from such contaminations, leading to accurate experimental results. In this scope, five highly isotopically enriched Ge samples have been used in this work. The quasi-monoenergetic neutron beams were produced via the $^3\text{H}(d,n)^4\text{He}$ reaction at the 5.5 MV Tandem Van de Graaff accelerator of N.C.S.R. ‘Demokritos’. The cross section of these nine reactions were measured using the activation method, with respect to the $^{27}\text{Al}(n,\alpha)^{24}\text{Na}$ reference reaction.

1 Introduction

Neutron induced cross section measurements on Ge isotopes are of major importance regarding both practical applications as well as fundamental research in the Nuclear Physics field. Practical applications include dosimetry, nuclear medicine, astrophysical projects and reactor technology [1–3]. Ge is also widely used in detectors for γ -ray spectroscopy. Furthermore, Ge is a very important material in semi-conductor technology, thus the investigation of its behavior in a neutron field is of considerable significance in these practical applications. Concerning fundamental nuclear physics research, some (n,x) reaction channels on Ge isotopes produce residual nuclei in high spin isomeric states, the population of which is governed by the spin distribution of the continuum phase space and the spins of the discrete levels involved [1, 4, 5]. The experimental determination of cross sections in reaction channels that produce such residual nuclei, can play a very important role in the study of the compound nucleus evaporation. Neutron induced reactions on the five isotopes of Ge yield a plethora of different reaction channels, revealing very interesting systematics, crucial for the optimization of the input parameters of statistical model calculations. These optimized parameters should simultaneously reproduce the population of isomeric and normal states as well as many other competing reaction channels,

acting as a very important constraint to statistical model calculations. Furthermore, in the energy region above 15 MeV, pre-equilibrium effects in the de-excitation of the compound nucleus become more significant [1], rendering the provided data in this energy region very important.

In the past, (n,x) reactions on Ge isotopes have been studied by the Nuclear Physics Group of the National Technical University of Athens [6, 7], by means of the $^2\text{H}(d,n)^3\text{He}$ reaction, producing quasi-monoenergetic neutron beams in the energy range 8-11.4 MeV. Furthermore, the existing experimental data in literature [8] for many reaction channels, cover a wide energy range, but they are discrepant and scarce especially in the region above 15 MeV. The majority of the aforementioned datasets implement ^{nat}Ge targets for the cross section measurements. In this case, for many reaction channels, the residual nucleus can be produced not only from the measured reaction, but also from “parasitic” or “interfering” reactions from neighboring isotopes that inevitably exist in the ^{nat}Ge target in their natural abundance. To compensate for these parasitic contributions, theoretical corrections accompanied by their own uncertainties should be applied. On the contrary, the use of isotopically enriched targets such as the ones implemented in this work, does not require such corrections, since no parasitic reactions take place, thus the provided data are more accurate and reliable.

* Corresponding author: sotirischasapoglou@mail.ntua.gr

2 Experimental Procedure

2.1 Targets

The targets used in the present work for the determination of the neutron induced cross sections, have been provided by the CERN n_TOF collaboration. Five isotopically enriched GeO₂ pellets of ^{70,72,73,74,76}Ge have been implemented with enrichment levels of 97.71, 96.59, 96.07, 95.51 and 88.46% respectively. The mass of each pellet was ~2 g. Each pellet was glued on a thin mylar foil, which in turn was glued on an Al ring. High purity Al metallic reference foils were also used for the determination of the neutron flux in the Ge targets. All Ge targets and Al reference foils had a diameter of 20 mm.

2.2 Neutron facility

The irradiations were carried out at the neutron production facility of the 5.5 MV Tandem Van de Graaf accelerator of N.C.S.R. “Demokritos” [9, 10] in Athens, Greece. The quasi-monoenergetic neutron beams were produced via the ³H(d,n)⁴He reaction. Deuteron beams impinged on a solid Ti-tritiated (TiT) target of 373 GBq activity. In front of the solid TiT target a 10 μm Mo foil was placed, where the deuteron beam lost part of its energy. The TiT target consists of a 2.1 mg/cm² Ti-tritiated layer on a 1 mm thick Cu backing for good heat conduction. The flange with the tritium target assembly was air cooled during the deuteron irradiation. The monoisotopic Ge pellets and reference foils were placed at a distance of ~2.4 cm from the flange with the Ti-T target, thus limiting the angular acceptance to ±19°, where the neutron beam can practically be considered as monoenergetic according to the reaction kinematics.

2.3 Irradiations

The duration of the irradiations varied between 5 and 25 hours, depending on the half-life of the measured isotope, while the fluctuations of the neutron beam were continuously monitored with a BF₃ detector. This detector was placed at ~3 m distance from the neutron producing target, at an angle with respect to the neutron beam, to minimize the neutron scattering. The corresponding spectra were saved at regular time intervals (~300 s) in a separate ADC during the irradiation in order to use the beam instabilities in the offline analysis to correct for the decay of the product nuclei during the irradiation.

In each irradiation, two Al foils were used to obtain the absolute value of the neutron flux using the well-known ²⁷Al(n,α)²⁴Na reference reaction.

After each irradiation, the induced radioactivity of the samples was measured with the use of HPGe detectors properly shielded and calibrated with a ¹⁵²Eu source placed at the same position as the irradiated samples. The activity measurements of the Ge and reference samples were carried out at a distance of 10 cm from the detector window, to avoid significant pile-up or true coincidence summing-effect corrections. The

yield of the characteristic transitions of each reaction was corrected for self-absorption and counting geometry of the emitted γ-rays in the irradiated sample, using Monte Carlo simulations.

3 Data analysis

3.1 Cross section calculation

The cross section calculation for the reactions involved in this work, is based on the following formula:

$$\sigma = \sigma_{\text{ref}} \cdot \frac{N_{\gamma,\text{tar}}}{N_{\gamma,\text{ref}}} \cdot \left[\frac{(\epsilon F I_{\gamma} D f_c N_t)_{\text{ref}}}{(\epsilon F I_{\gamma} D f_c N_t)_{\text{tar}}} \right] \cdot \frac{\Phi_{\text{ref}}}{\Phi_{\text{tar}}} \quad (1)$$

Where the subscripts “ref” and “tar” refer to the reference foils and measured targets, respectively. Concerning the rest of the factors in eq. (1):

- σ is the cross section measured in barns. For the ²⁷Al(n,α)²⁴Na reference reaction, the cross section value was obtained from the ENDF/B-VIII.0 library [11]
- N_{γ} is the γ-ray peak integral from the spectrum obtained by the HPGe detector. The obtained γ-ray spectra (such as the one shown in Fig. 1 for the irradiation of the ⁷³Ge sample), were analyzed via the “Tv” software [12]
- ϵ is the absolute efficiency of the HPGe detector at the characteristic γ-ray energy
- I_{γ} is the γ-ray intensity
- D is a correction factor for the de-excitation of the residual nuclei during the cooling time (t_1) between the end of the irradiation and the start of the measurement in the HPGe detector, and during the measurement itself in front of the HPGe detector (t_2). This correction factor is given by the expression $D = \exp(-\lambda t_1) - \exp(-\lambda t_2)$
- f_c is a correction factor for the decaying nuclei produced during the irradiation time (t_b), taking into account the fluctuations of the neutron beam. This correction factor is given by the expression: $f_c = \frac{\int_0^{t_b} e^{\lambda t} f(t) dt}{\int_0^{t_b} f(t) dt} \cdot e^{-\lambda t_b}$, where the factor $f(t)$ represents the counts obtained from the BF₃ detector, stored in dt time intervals.
- N_t is the number of total nuclei of the measured isotope in the target
- $\Phi_{\text{ref}}/\Phi_{\text{tar}}$ is the neutron flux ratio for the reference foil and the measured target respectively. This ratio was calculated via the combined use of NeusSDesc [13, 14] and MCNP5 [15] Monte Carlo codes.

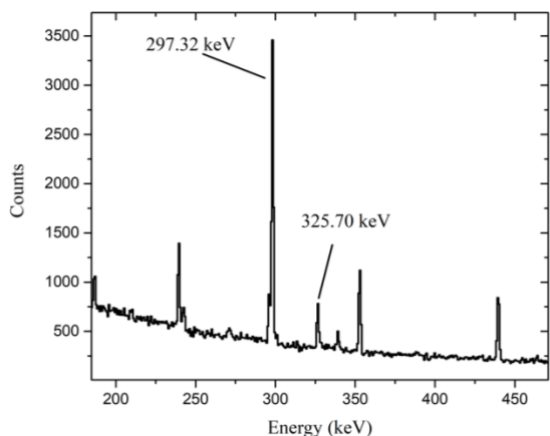


Fig. 1 A typical γ -ray spectrum obtained from a HPGe detector. The most intense γ -rays from the ^{73}Ga residual nucleus following the $^{73}\text{Ge}(n,p)^{73}\text{Ga}$ reaction, are displayed in the spectrum. The total number of channels in the spectrum was 4096, with the keV/channel being 0.73.

3.2 Monte Carlo simulations

Monte Carlo simulations were performed by means of the NeuSDesc and MCNP5 codes, in order to calculate the propagation of the neutron beam through the consecutive Ge targets and reference foils. Firstly, the neutron source was produced as an SDEF card from the NeuSDesc code, taking into account the physical and geometrical characteristics of the neutron producing target. Then this SDEF card was fed into the MCNP5 code, in which the detailed geometry of the experiment was described, as seen in Fig. 2. Finally, the neutron flux was calculated in every Ge target and reference foil of the experiment.

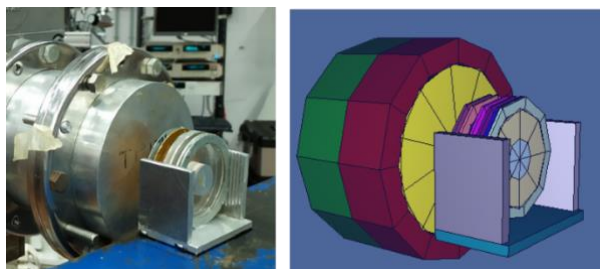


Fig. 2 Monte Carlo visualisation of the Al flange for the Tritiated target, the target assembly and its holder

A typical MCNP5 output can be seen in Fig. 3., where the neutron flux was scored in every Al reference foil (Al1 and Al2) as well as in the two Ge targets (^{72}Ge and ^{74}Ge) that were simultaneously irradiated.

The shape of the neutron flux, as seen in Fig. 3, is not purely monoenergetic, having a mean value 17.9 MeV at the nominal neutron energy and energy dispersion of ± 0.3 MeV. It is also followed by a low energy parasitic neutron tail with intensity lower by 2-3 orders of magnitude. Since the reactions studied in this work have thresholds in the MeV region, this low energy neutron tail does not interfere with the measured yield.

The factor $\Phi_{\text{ref}}/\Phi_{\text{tar}}$ of eq. 1 is calculated from the ratio of the integrals of the main peaks of the neutron flux for the reference foil and measured target, respectively.

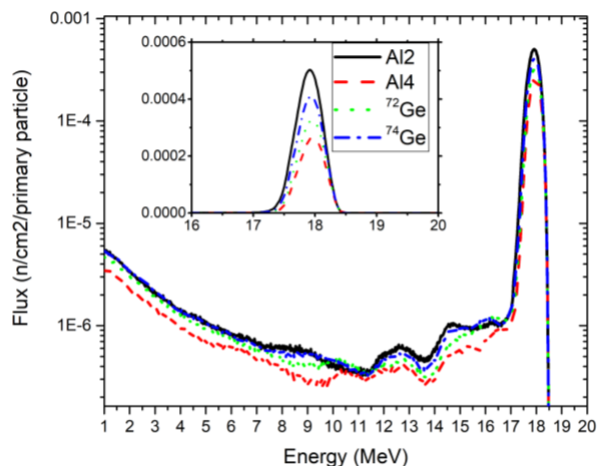


Fig. 3 Typical flux obtained from the MCNP5 simulations at the reference foils and Ge targets. The targets were placed between two Al reference foils. Al2 was placed in the front of the ^{74}Ge and Al4 at the back of the ^{72}Ge targets.

4 Preliminary results & discussion

In this section, the preliminary results of the $^{70}\text{Ge}(n,2n)^{69}\text{Ge}$, $^{76}\text{Ge}(n,2n)^{75}\text{Ge}$, $^{73}\text{Ge}(n,p)^{73}\text{Ga}$, $^{72}\text{Ge}(n,p)^{72}\text{Ga}$, $^{73}\text{Ge}(n,d/np)^{72}\text{Ga}$, $^{74}\text{Ge}(n,d/np)^{73}\text{Ga}$, $^{74}\text{Ge}(n,\alpha)^{71\text{m}}\text{Zn}$, $^{72}\text{Ge}(n,\alpha)^{69\text{m}}\text{Zn}$, $^{73}\text{Ge}(n,\alpha)^{69\text{m}}\text{Zn}$ reaction cross sections will be presented. For clarity reasons, in all the relevant figures (Fig. 4, Fig. 5, Fig. 6, Fig. 7, Fig. 10, Fig. 11), the experimental points retrieved from the EXFOR database are presented in grey. Only the ones discussed in the manuscript are presented in blue or black.

4.1 The $^{70}\text{Ge}(n,2n)^{69}\text{Ge}$ reaction

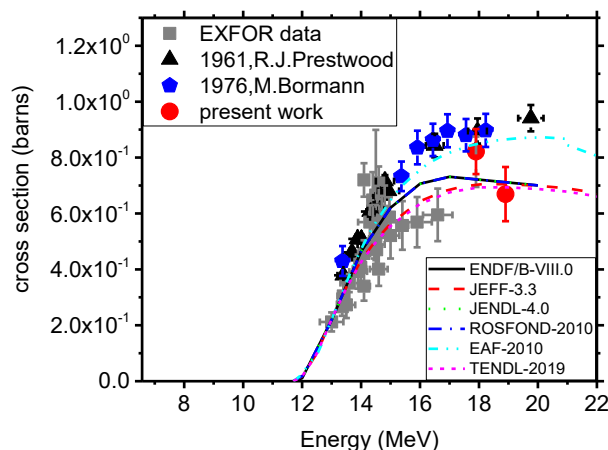


Fig. 4 The $^{70}\text{Ge}(n,2n)^{69}\text{Ge}$ reaction cross section results of the present work (red solid points), alongside with previous EXFOR data and evaluation curves (continuous and dashed lines).

The preliminary cross section results of the $^{70}\text{Ge}(n,2n)^{69}\text{Ge}$ reaction can be seen in Fig. 4 for neutron energies of 17.9 and 18.9 MeV. The residual nucleus ^{69}Ge decays with a half-life of 39.05h to ^{69}Ga which de-excites to its ground state through the characteristic gamma-rays 1106.7, 574.1 and 871.9 keV with

intensities 36%, 13.3% and 11.9%, respectively. The cross section points for both energies were calculated from the weighted average of the cross sections derived from the 574.1 and 871.9 keV lines which produced similar results, while the cross section value derived from the 1106.7 keV γ -ray was lower by $\sim 12\%$ and was neglected from the calculation. For the 17.9 MeV cross section point, the data of the present work seem to be in good agreement with the dataset of Bormann et al. [16] and Prestwood et al. [17] as well as with the EAF 2010 [18] evaluation library. The 18.9 MeV cross section point seems to be in good agreement with the ROSFOND 2010 [19], ENDF/B-VIII.0 [11], JEFF 3.3 [20], JENDL 4.0 [21] and TENDL 2019 [22]. Two general trends of the data appear for neutron energies above 14 MeV. These very large discrepancies could be attributed to the large errors of the γ -ray intensities that are found in literature and reach up to 13%. More experimental points in the energy region between 14 and 20 MeV are needed to solve these discrepancies.

4.2 The $^{76}\text{Ge}(n,2n)^{75}\text{Ge}$ reaction

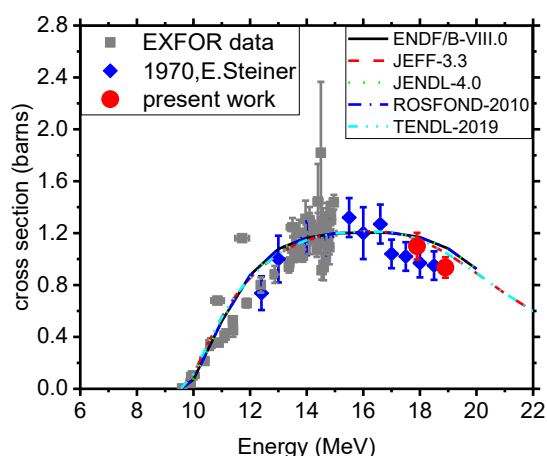


Fig. 5 The $^{76}\text{Ge}(n,2n)^{75}\text{Ge}$ reaction cross section results of the present work (red solid points), alongside with previous EXFOR data and evaluation curves (continuous and dashed lines).

The preliminary cross section results of the $^{76}\text{Ge}(n,2n)^{75}\text{Ge}$ reaction can be seen in Fig. 5 for neutron energies of 17.9 and 18.9 MeV. This reaction leads to the formation of the unstable residual nucleus ^{75}Ge both in its $1/2^-$ ground state with half-life 82.78 min and its metastable $7/2^+$ state with half-life 47.7 s. The de-excitation of the metastable to the ground state in fraction 99.97%, along with its short lifetime leads to the measurement of the total cross section σ_{m+g} , corresponding to the production of both ground and metastable states of the $(n,2n)$ reaction, via the 264.6 keV (with intensity 11.4%) characteristic transition of ^{75}As . For both energies, the cross section results of the present work are in very good agreement with the only existing dataset of Steiner et al. [23] in this energy region, within the experimental uncertainties. The present data are also in fair agreement with the existing evaluation libraries [11, 19–22].

4.3 The $^{72}\text{Ge}(n,p)^{72}\text{Ga}$ reaction

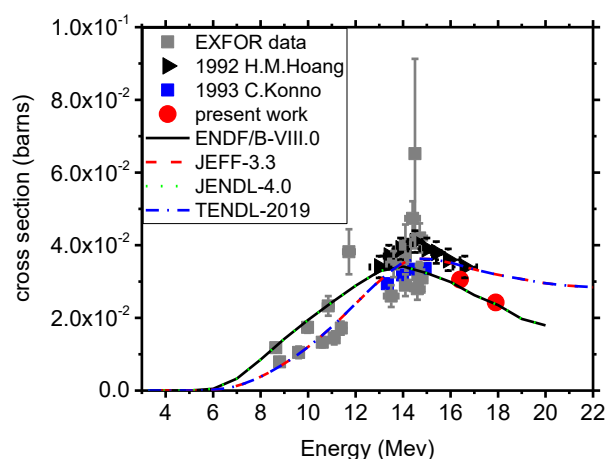


Fig. 6 The $^{72}\text{Ge}(n,p)^{72}\text{Ga}$ reaction cross section results of the present work (red solid points), alongside with previous EXFOR data and evaluation curves (continuous and dashed lines).

The preliminary cross section results of the $^{72}\text{Ge}(n,p)^{72}\text{Ga}$ reaction can be seen in Fig. 6 for neutron energies of 16.4 and 17.9 MeV. The produced nucleus ^{72}Ga decays with a half-life of 14.1 h to ^{72}Ge , whose de-excitation to its ground state proceeds through the 834.1, 629.9 and 894.33 keV gamma-rays of 95.45%, 26.13% and 10.14% intensity, respectively. The cross-section results were calculated from the weighted average of the three aforementioned γ -rays, and seem to be in good agreement with the lower trend of existing data, also followed by Konno et al. [24] (that also used an enriched target) as well as with the ENDF/B-VIII.0 and JENDL 4.0 evaluation libraries. There are no existing experimental data above 15 MeV except the ones from Hoang et al. [25], while the data in lower energies exhibit discrepancies among them. In this reaction, two general trends are followed from the different evaluation libraries. These discrepancies could possibly be attributed to the different methodologies followed for the subtraction of the parasitic reaction contribution in the case of the ^{nat}Ge target, used in most of the experiments.

4.4 The $^{73}\text{Ge}(n,p)^{73}\text{Ga}$ reaction

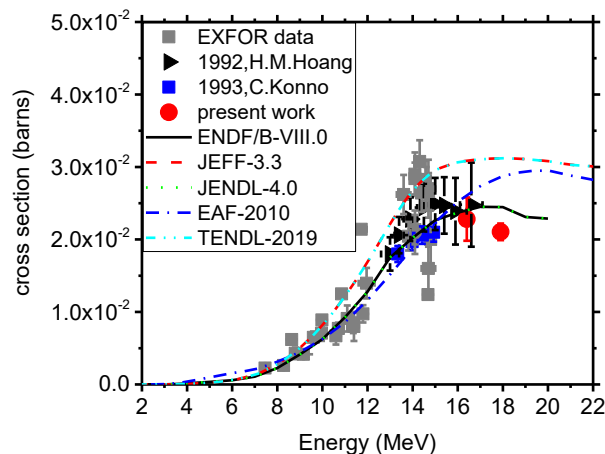


Fig. 7 The $^{73}\text{Ge}(n,p)^{73}\text{Ga}$ reaction cross section results of the present work (red solid points), alongside with previous EXFOR data and evaluation curves (continuous and dashed lines).

The preliminary cross section results of the $^{73}\text{Ge}(n,p)^{73}\text{Ga}$ reaction can be seen in Fig. 7 for neutron energies of 16.4 and 17.9 MeV. The residual nucleus ^{73}Ga decays with a lifetime of 4.86 h to ^{73}Ge whose de-excitation involves the 297.3 keV characteristic gamma-ray of 79.8% intensity. The experimental data of this work are in fair agreement with the trends of the datasets of Hoang et al. [25] and Konno et al. [24] (that also used an enriched target) within their experimental uncertainties. The trend of the JENDL 4.0 and ENDF/B-VIII.0 evaluations follow the data of the present work but seem to be slightly overestimated. There is also lack of experimental data above 14 MeV, while very large discrepancies exist even at lower energies. These discrepancies can be attributed to the fact that the vast majority of the cross section data found in literature were measured with the use of a ^{nat}Ge target, so theoretical corrections should be applied for the subtraction of parasitic reactions from neighboring isotopes found in the ^{nat}Ge target in their natural abundances, that lead to the formation of the same residual nucleus, acting as a contamination to the measured yield. The accuracy of the methodologies followed for these corrections should be checked, especially at neutron energies above 14 MeV.

4.5 The $^{73}\text{Ge}(n,d/np)^{72}\text{Ga}$ reaction

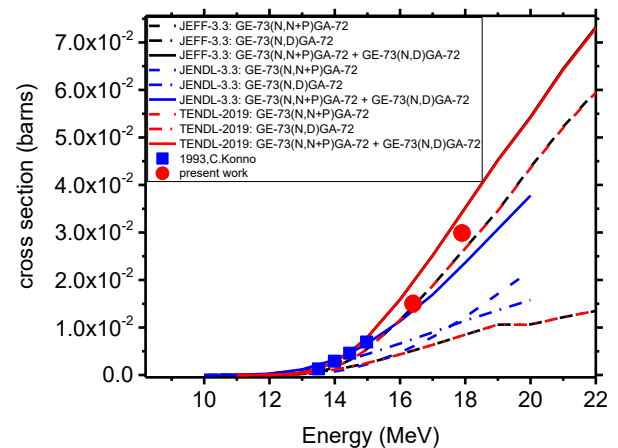


Fig. 8 The $^{73}\text{Ge}(n,d/np)^{72}\text{Ga}$ cross section results of the present work (red solid points), alongside with previous EXFOR data and evaluation curves (continuous and dashed lines).

The preliminary results for the $^{73}\text{Ge}(n,d/np)^{72}\text{Ga}$ can be seen in Fig. 8 for neutron energies of 16.4 and 17.9 MeV. The produced nucleus ^{72}Ga decays with a half-life of 14.1 h to ^{72}Ge , as described in detail in section 4.3. The residual nucleus ^{72}Ga is produced both from the $^{73}\text{Ge}(n,d)$ and the $^{73}\text{Ge}(n,np)$ reaction channels, that cannot be distinguished via the neutron activation method. For this reason, in Fig. 8, the sums of these two cross sections from the evaluation libraries are plotted as solid lines. The experimental data of this work for this challenging reaction are in very good agreement with the existing dataset of Konno et al., as well as with the trends of JENDL 3.3 [26] and TENDL 2019 [22] libraries. This reaction is very hard to study with the use of ^{nat}Ge target due to its low cross section and low natural abundance of the ^{73}Ge isotope.

4.6 The $^{74}\text{Ge}(n,d/np)^{73}\text{Ga}$ reaction

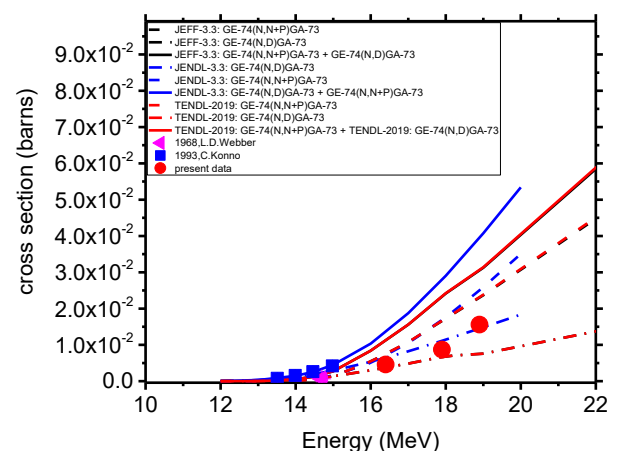


Fig. 9 The $^{74}\text{Ge}(n,d/np)^{73}\text{Ga}$ cross section results of the present work (red solid points), alongside with previous EXFOR data and evaluation curves (continuous and dashed lines).

The preliminary results for the $^{74}\text{Ge}(n,d/np)^{73}\text{Ga}$ reaction are presented in Fig. 9 for neutron energies of

16.4, 17.9 and 18.9 MeV. The decay of the residual nucleus ^{73}Ga is described in detail in section 4.4. This is another challenging reaction to study with a $^{\text{nat}}\text{Ge}$ target due to the significant contribution of the $^{73}\text{Ge}(n,p)^{73}\text{Ga}$ reaction to the measured yield. In the case of isotopically enriched targets, this contribution can be considered negligible. The $^{74}\text{Ge}(n,np)$ and the $^{74}\text{Ge}(n,d)$ reactions produce the same residual nucleus (^{73}Ga), so the measured cross section via the activation method refers to the sum of both reaction channels. The sum of these cross sections for the evaluation libraries JEFF 3.3 [20], JENDL 3.3 [26] and TENDL 2019 [22] are plotted in Fig. 9 with solid lines. The experimental data of the present work are in fair agreement with the dataset of Konno et al., while the existing libraries seem to overestimate the cross section values above 15 MeV.

4.7 The $^{72}\text{Ge}(n,\alpha)^{69\text{m}}\text{Zn}$ reaction

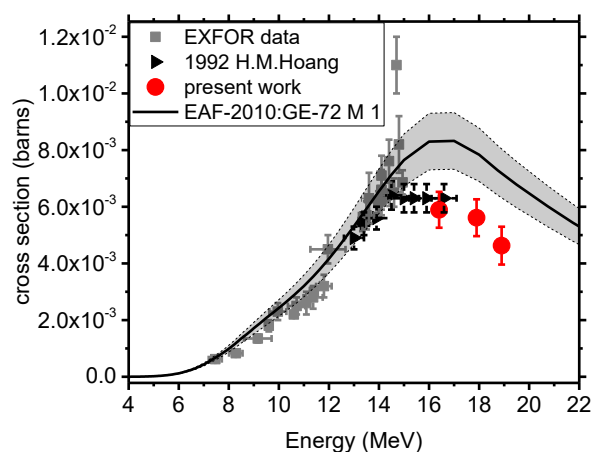


Fig. 10 The $^{72}\text{Ge}(n,\alpha)^{69\text{m}}\text{Zn}$ cross section results of the present work (red solid points), alongside with previous EXFOR data and evaluation curves (continuous and dashed lines).

The preliminary results for the $^{72}\text{Ge}(n,\alpha)^{69\text{m}}\text{Zn}$ reaction are presented in Fig. 10 for neutron energies of 16.4, 17.9 and 18.9 MeV. The residual nucleus ^{69}Zn is produced both in its $1/2^-$ ground state ($T_{1/2} = 56.4$ min) and its metastable $9/2^+$ ($T_{1/2} = 13.76$ h) state. The ground state of ^{69}Zn decays directly to the ground state of ^{69}Ga , while the metastable state decays to the ground state of ^{69}Zn through the emission of the characteristic 438.6 keV γ -ray, with intensity 94.85%, which has been used for the determination of the σ_m cross section. The trend followed by the experimental cross section points of the present work seem to be in very good agreement with the trend of EAF 2010 [18] evaluation library, the only one containing this reaction cross section values and uncertainties. However, this library seems to slightly overestimate the cross section in neutron energies above ~ 15 MeV. The cross section result for the 16.4 MeV neutron energy is in very good agreement with the only dataset in this energy range, by Hoang et al. [25]. More cross section points in neutron energies above 15 MeV would improve the accuracy and reliability of future evaluation curves.

4.8 The $^{74}\text{Ge}(n,\alpha)^{71\text{m}}\text{Zn}$ reaction

The preliminary results for the $^{74}\text{Ge}(n,\alpha)^{71\text{m}}\text{Zn}$ reaction can be seen in Fig. 11 for neutron energies 16.4 and 17.9 MeV. The residual nucleus ^{71}Zn is produced both in its $1/2^-$ ground state ($T_{1/2} = 2.45$ m) and its metastable $9/2^+$ ($T_{1/2} = 3.96$ h) state. Due to the short lifetime of the ground state of ^{71}Zn , only the activity of the metastable state could be measured via the activation technique. Thus, the σ_m was determined via the 386.28 keV (with intensity 91.4%) transition of ^{71}Ga which is fed by the decay of the metastable state of ^{71}Zn . For the 16.4 MeV neutron energy, the cross section measurements of the present work are in very good agreement with the dataset of Hoang et al. [25], which is the only one providing data at neutron energies above 15 MeV. The cross section data are in very good agreement with the EAF 2010 evaluation library. In Fig. 10, the error bands of the JEFF 3.3, EAF 2010 and TENDL 2019 libraries are also plotted to indicate the existing uncertainties and discrepancies among the evaluation libraries. Accurate experimental cross section data, such as the ones produced from enriched targets, could vastly improve the accuracy of future evaluations.

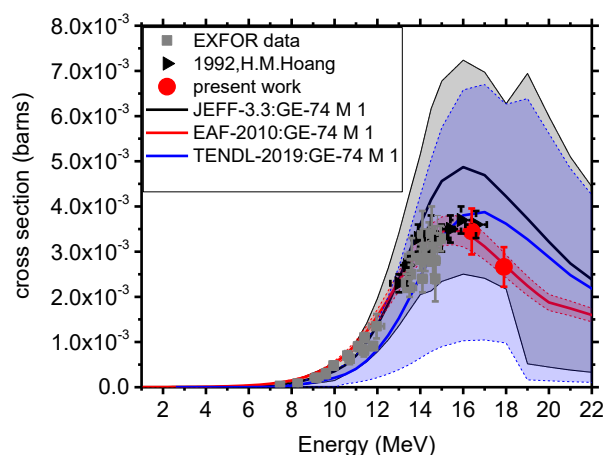


Fig. 11 The $^{74}\text{Ge}(n,\alpha)^{71\text{m}}\text{Zn}$ cross section results of the present work (red solid points), alongside with previous EXFOR data and evaluation curves (continuous and dashed lines).

4.9 The $^{73}\text{Ge}(n,n\alpha)^{69\text{m}}\text{Zn}$ reaction

The preliminary results for the $^{73}\text{Ge}(n,n\alpha)^{69\text{m}}\text{Zn}$ reaction along with evaluation libraries can be seen in Fig. 12, displaying large uncertainties reaching up to more than 70% in some energies. The residual nucleus ^{69}Zn is produced both in its $1/2^-$ ground state ($T_{1/2} = 56.4$ min) and its metastable $9/2^+$ ($T_{1/2} = 13.76$ h) state, and its decay is described in section 4.7. There were no other experimental data found in literature since this is a very challenging reaction to study with a $^{\text{nat}}\text{Ge}$ target (which are the ones most commonly found in literature) due to the low natural abundance of the ^{73}Ge isotope (7.76 %) and the low cross section of this reaction. The experimental cross section points of this work follow the trend of the JEFF 3.3, EAF 2010 and TENDL 2019 libraries and their values within their uncertainties. Accurate cross section data in such a challenging reaction could improve future evaluation curves.

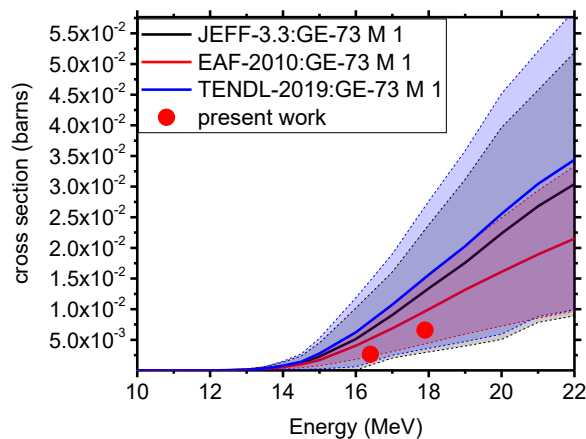


Fig. 12 The $^{73}\text{Ge}(n,\alpha)^{69m}\text{Zn}$ reaction results of the present work (red solid points), alongside with previous EXFOR data and evaluation curves (continuous and dashed lines).

5 Summary & conclusions

The cross sections of the $^{70}\text{Ge}(n,2n)^{69}\text{Ge}$, $^{76}\text{Ge}(n,2n)^{75}\text{Ge}$, $^{73}\text{Ge}(n,p)^{73}\text{Ga}$, $^{72}\text{Ge}(n,p)^{72}\text{Ga}$, $^{73}\text{Ge}(n,d/np)^{72}\text{Ga}$, $^{74}\text{Ge}(n,d/np)^{73}\text{Ga}$, $^{74}\text{Ge}(n,\alpha)^{71m}\text{Zn}$, $^{72}\text{Ge}(n,\alpha)^{69m}\text{Zn}$ and $^{73}\text{Ge}(n,\alpha)^{69m}\text{Zn}$ reactions have been measured at neutron energies of 16.4, 17.9 and 18.9 MeV employing highly enriched Ge targets that were provided by the CERN n_TOF collaboration and the preliminary results of these cross sections are presented. The experimental cross sections were measured at neutron energies where only a few and often discrepant data exist in literature. The use of enriched isotopes produce more accurate cross section results in comparison with the ones obtained from ^{nat}Ge targets. In the case of ^{nat}Ge targets, neutron induced reactions in neighboring isotopes that are found in the ^{nat}Ge target in their natural isotopic abundance, could lead to the production of the same residual nucleus, as the one produced from the measured reaction, acting as a contamination. In this scope, theoretical corrections, that bear their own uncertainties, should be applied. The contribution of these parasitic reactions becomes larger for energies above 14 MeV where very few experimental data points exist. Enriched targets on the other hand, do not suffer from such contaminations, enabling accurate measurements even at higher neutron energies above 14 MeV. These accurate cross section results in a plethora of reaction channels on Ge isotopes could act as a very important constraint in statistical model calculations, via the simultaneous reproduction of all of these channels, using the same set of input parameters. These parameters could also be applied in other medium-heavy nuclei in the same mass region. As a consequence, despite their high cost and difficulty to obtain, cross section measurements with isotopically enriched targets in key medium-heavy even-even nuclei (such as Ge with many natural isotopes that could lead to parasitic reactions) and in strategical energies could significantly improve the accuracy of future evaluation curves and statistical model calculations.

Acknowledgments

We acknowledge support of this work by the project CALIBRA/EYIE (MIS 5002799), which is implemented under the Action “Reinforcement of the Research and Innovation Infrastructures”, funded by the Operational Program “Competitiveness, Entrepreneurship and Innovation” (NSRF 2014-2020) and co-financed by Greece and the European Union (European Regional Development Fund)

The research work was supported by the Hellenic Foundation for Research and Innovation (HFRI) under the 3rd Call for HFRI PhD Fellowships (Fellowship Number: 5597).

We gratefully acknowledge the financial support by the PEVE 2021 project of NTUA.

References

- Avriganu M, Avriganu V, Diakaki M, Vlastou R (2012) Isomeric cross sections of fast-neutron-induced reactions on 197 Au. *Phys Rev C* 85:44618. <https://doi.org/10.1103/PhysRevC.85.044618>
- Fessler A, Plompen AJM, Smith DL, et al (2000) Neutron activation cross-section measurements from 16 to 20 MeV for isotopes of F, Na, Mg, Al, Si, P, Cl, Ti, V, Mn, Fe, Nb, Sn, and Ba. *Nucl Sci Eng* 134:171–200. <https://doi.org/10.13182/NSE99-14>
- Talou P, Kawano T, Young PG, et al (2007) Improved evaluations of neutron-induced reactions on americium isotopes. *Nucl Sci Eng* 155:84–95. <https://doi.org/10.13182/NSE07-A2646>
- Dzysiuk N, Koning A (2017) Improving activation cross section data with TALYS. *EPJ Web Conf* 146:2047. <https://doi.org/10.1051/epjconf/201714602047>
- Tsinganis A, Diakaki M, Kokkoris M, et al (2011) Isomeric cross section of the 197 Au(n,2n) reaction. *Phys Rev C* 83:24609. <https://doi.org/10.1103/PhysRevC.83.024609>
- Vlastou R, Papadopoulos CT, Kokkoris M, et al (2007) Neutron induced reactions at the Athens Tandem Accelerator NCSR “Demokritos.” *J Radioanal Nucl Chem* 272:219–222. <https://doi.org/10.1007/s10967-007-0503-8>
- Galanopoulos S, Vlastou R, Papadopoulos CT, et al (2007) Experimental and theoretical studies of (n, p) reactions on Ge isotopes. *Nucl Instruments Methods Phys Res Sect B Beam Interact with Mater Atoms* 261:969–973. <https://doi.org/10.1016/j.nimb.2007.04.007>
- Otuka N, Dupont E, Semkova V, et al (2014) Towards a More Complete and Accurate Experimental Nuclear Reaction Data Library (EXFOR): International Collaboration Between Nuclear Reaction Data Centres (NRDC). *Nucl Data Sheets* 120:272–276. <https://doi.org/https://doi.org/10.1016/j.nds.201>

- 4.07.065
9. Vlastou R, Kokkoris M, Diakaki M, et al (2011) Characterization of the neutron flux distribution at the Athens Tandem Accelerator NCSR “demokritos.” In: Nuclear Instruments and Methods in Physics Research, Section B: Beam Interactions with Materials and Atoms. North-Holland, pp 3266–3270
 10. Kalamara A, Patronis N, Vlastou R, et al (2019) Determination of the $^{193}\text{Ir}(n, 2n)$ reaction cross section and correction methodology for the $^{191}\text{Ir}(n, \gamma)$ contamination. *Eur Phys J A* 55:1–11. <https://doi.org/10.1140/epja/i2019-12879-x>
 11. Brown DA, Chadwick MB, Capote R, et al (2018) ENDF/B-VIII.0: The 8th Major Release of the Nuclear Reaction Data Library with CIELO-project Cross Sections, New Standards and Thermal Scattering Data. *Nucl Data Sheets* 148:1–142. <https://doi.org/10.1016/j.nds.2018.02.001>
 12. Theuerkauf J, Esser S, Krink S, et al Program Tv
 13. Birgersson E, Lövestam G NeuSDesc-Neutron Source Description Software Manual
 14. Evert B, Goeran L (2009) NeuSDesc-Neutron Source Description Software Manual. Tech Report, EUR 23794 EN (European Com
 15. Team X-5 MC (2003) MCNP—version 5, Vol. I: Overview and theory. LA-UR-03-1987, Los Alamos Natl. Lab.
 16. Bormann M, Feddersen H-K, Hölscher H-H, et al (1976) $(n, 2n)$ Anregungsfunktionen für ^{54}Fe , ^{70}Ge , ^{74}Se , ^{85}Rb , ^{86}Sr , ^{89}Y , ^{92}Mo , ^{204}Hg im Neutronenenergiebereich 13–18 MeV. *Zeitschrift für Phys A Atoms Nucl* 277:203–210. <https://doi.org/10.1007/BF01433714>
 17. Prestwood RJ, Bayhurst BP (1961) $(n, 2n)$ Excitation Functions of Several Nuclei from 12.0 to 19.8 Mev. *Phys Rev* 121:1438–1441. <https://doi.org/10.1103/PhysRev.121.1438>
 18. Sublet J-C, Packer LW, Kopecky J, et al EASY Documentation Series The European Activation File: EAF-2010 neutron-induced cross section library
 19. Zabrodszkaya S V, Ignatyuk A V, Koscheev VN (2007) ROSFOND - Rossiyskaya Natsionalnaya Biblioteka Nejtronnykh Dannykh. Ross Natsionalnaya Bibl Nejtr Dannykh, VANT, *Nucl Constants* 3:1–2
 20. Plompen AJM, Cabellos O, De Saint Jean C, et al (2020) The joint evaluated fission and fusion nuclear data library, JEFF-3.3. *Eur Phys J A* 56:181. <https://doi.org/10.1140/epja/s10050-020-00141-9>
 21. Shibata K, Iwamoto O, Nakagawa T, et al (2011) JENDL-4.0: A new library for nuclear science and engineering. *J Nucl Sci Technol* 48:1–30. <https://doi.org/10.1080/18811248.2011.9711675>
 22. Koning AJ, Rochman D, Sublet J-C, et al (2019) TENDL: Complete Nuclear Data Library for Innovative Nuclear Science and Technology. *Nucl Data Sheets* 155:1–55. <https://doi.org/https://doi.org/10.1016/j.nds.2019.01.002>
 23. E.Steiner, P.Huber, W.Salathe RW (1970) $(n,2n)$ cross-sections and isomer cross-section ratios of Ge-76 and Ho-165 in the energy range from 12.5 to 18.5 MeV. *Helv Phys Acta* 43:17
 24. Konno C, Ikeda Y, Kawade K, et al (1993) Activation cross section measurements at neutron energy from 13.3 to 14.9 MeV using the FNS facility. *Jaeri*
 25. Hoang HM, Garuska U, Kielan D, et al (1992) Energy dependence of the isotopic effect in the (n,p) reaction on the germanium isotopes. *Zeitschrift für Phys A Hadron Nucl* 342:283–290. <https://doi.org/10.1007/BF01291511>
 26. SHIBATA K, KAWANO T, NAKAGAWA T, et al (2002) Japanese Evaluated Nuclear Data Library Version 3 Revision-3: JENDL-3.3. *J Nucl Sci Technol* 39:1125–1136. <https://doi.org/10.1080/18811248.2002.9715303>